# A REPRESENTATION OF ACOUSTIC WAVES IN UNBOUNDED DOMAINS

BRADLEY K. ALPERT AND YU CHEN

ABSTRACT. Compact, time-harmonic, acoustic sources produce waves that decay too slowly to be square-integrable on a line away from the sources. We introduce an inner product, arising directly from Green's second theorem, to form a Hilbert space of these waves, and present examples of its computation.

## 1. INTRODUCTION

Consider the scattering problem governed by the Helmholtz equation

$$\Delta\varphi + k^2(1+q)\varphi = 0 \tag{1}$$

in two dimensions for a scatterer $q \in L^2(D)$ supported in a compact domain $D$ in the half plane above the $x$-axis. A function $u : \mathbb{R}^2 \to \mathbb{C}$ is referred to as a scattered wave, or an outgoing wave, from $D$ if it has the form

$$u(\mathbf{r}) = \int_D H_0(k|\mathbf{r}-\mathbf{r}'|)\,\eta(\mathbf{r}')\,d\mathbf{r}' \tag{2}$$

for some $\eta \in L^2(D)$. (We write $H_n$ for the Hankel function $H_n^{(1)}$.) As is well known, $u$ satisfies the radiation condition

$$\frac{\partial u}{\partial r} - iku = o(r^{-1/2}), \qquad r = |\mathbf{r}|, \tag{3}$$

and when restricted to a line such as the $x$-axis (see Figure 1), $u$ decays at the rate of $O\left(r^{-1/2}\right)$. Therefore $u$ is not an $L^2$ function and we cannot apply the standard inner product

$$(f,g) = \int_{-\infty}^{\infty} f(x)\,\bar{g}(x)\,dx. \tag{4}$$

There are several applications for which an outgoing wave may need to be sampled and processed on a line. First, for wave scattering or propagation problems in a stratified host medium or in a wave guide, we may have to process wave functions on a line in two dimensions, or a plane in three dimensions. Secondly, even if we do not have to deal with the wave functions on a line, it may be simpler, more convenient, or more efficient to discretize them there, as well as in $D$, in order

*Date*: October 15, 2002.



Research supported in part by DARPA Applied and Computational Mathematics Program, appropriation 9720400 (BKA) and Office of Naval Research, contract N00014-98-1-0514 (YC).

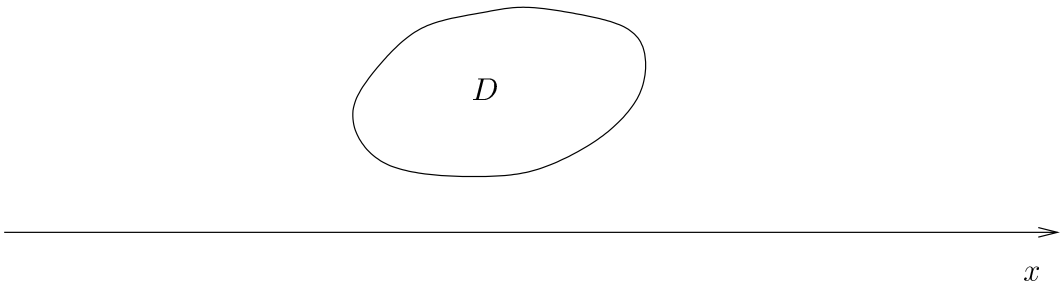



FIGURE 1. The scatterer $D$ above the $x$-axis.

to solve the related scattering problems. Finally, we may begin with a scatterer in a homogeneous host medium, but it may be again more simple, convenient, efficient, or stable to deal with the scattered wave on a line, as opposed to a closed curve containing $D$.

The lack of compact support of such functions makes their sampling and processing seem difficult. We introduce in this paper an inner product and use it to construct an orthogonal basis for all outgoing waves from $D$. In other words, we will present a method to efficiently sample the outgoing wave functions on the line.

## 2. The Inner Product

For simplicity, we will assume that the domain $D$ is a positive distance from, as well as above, the $x$-axis; see Figure 1 and Remark 2.4. Denote by $\mathcal{W}$ the linear space of functions that are restrictions to the $x$-axis of the outgoing waves $u(x, y)$ from $D$. In other words, let $A : L^2(D) \to C^\infty(\mathbb{R})$ be defined by

$$u(x) = (A\eta)(x) := \int_D H_0(k\rho)\, \eta(x', y')\, dx'\, dy' \tag{5}$$

with

$$\rho = \left[ (x - x')^2 + {y'}^2 \right]^{1/2}.$$

Then $\mathcal{W}$ is the range space of $A$. With the negative $y$-direction as the outward normal, we will denote by $u_n(x)$ the normal derivative of $u$ on the $x$-axis:

$$\begin{aligned} u_n(x) &= -\int_D \left. \frac{\partial H_0\left(k\sqrt{(x-x')^2 + (y-y')^2}\right)}{\partial y} \right|_{y=0} \eta(x', y')\, dx'\, dy' \\ &= -\int_D k\, H_1(k\rho)\, \frac{y'}{\rho}\, \eta(x', y')\, dx'\, dy'. \end{aligned}$$

Therefore, for any $u \in \mathcal{W}$,

$$u(x) = O(|x|^{-1/2}), \qquad u_n(x) = O(|x|^{-3/2}). \tag{6}$$

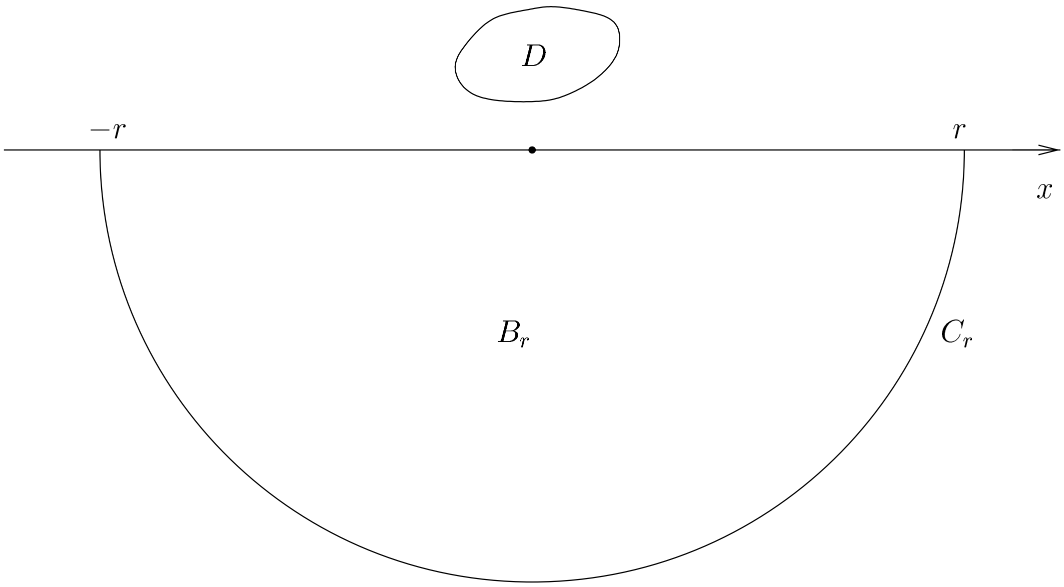


FIGURE 2. The scatterer $D$, semicircle $C_r$, and half disk $B_r$.

**Theorem 2.1.** *For $u$, $v \in \mathcal{W}$, the bilinear form*

$$(u, v) = \frac{i}{4} \int_{\mathbb{R}} [u(x)\, \bar{v}_n(x) - \bar{v}(x)\, u_n(x)]\, dx \tag{7}$$

*is bounded and defines an inner product for $\mathcal{W}$.*

*Proof.* The existence of the integral for $(u, v)$ follows immediately from (6). The bilinearity and symmetry of $(u, v)$ are straightforward to verify. Now, we establish the positivity $(u, u) > 0$ for a nonvanishing $u \in \mathcal{W}$. In the lower half plane consider the semicircle

$$C_r = \{\, (x, y) \mid x^2 + y^2 = r^2,\ y \leq 0 \,\} \tag{8}$$

and the half disk $B_r$ bounded by $C_r$ and the interval $[-r, r]$ on the $x$-axis; see Figure 2. Let $v = \bar{u}$ in Green's second theorem

$$\int_{B_r} \left[u \cdot (\Delta + k^2)v - v \cdot (\Delta + k^2)u\right] dx\, dy = \int_{\partial B_r} \left( u\, \frac{\partial v}{\partial n} - v\, \frac{\partial u}{\partial n} \right) ds, \tag{9}$$

where $u(x, y)$ on $B_r$ is the continuation of $u(x)$ on the line to the lower half plane; see (2) and (5). It follows from $(\Delta + k^2)\bar{u} = 0$ in $B_r$ that

$$\int_{-r}^{r} [u\, \bar{u}_n - \bar{u}\, u_n]\, dx = \int_{C_r} \left[ u\, \frac{\partial \bar{u}}{\partial n} - \bar{u}\, \frac{\partial \bar{u}}{\partial n} \right] ds. \tag{10}$$

The last integral we denote by $I(r)$. Integrating the radiation condition (3) over $C_r$ yields

$$\int_{C_r} \left| \frac{\partial u}{\partial n} - iku \right|^2 ds = \int_{C_r} \left[ \left| \frac{\partial u}{\partial n} \right|^2 + k^2 |u|^2 \right] ds - ikI(r) \to 0, \quad r \to \infty. \tag{11}$$

It follows from (7), (10), and (11) that

$$(u,u) = \frac{1}{4k} \lim_{r\to\infty} \int_{C_r} \left[ \left| \frac{\partial u}{\partial n} \right|^2 + k^2 |u|^2 \right] ds. \tag{12}$$

Therefore, $(u,u) = 0$ implies that the 2-norm over $[\pi, 2\pi]$ of the far field $u_\infty(\theta)$ is zero. It follows from the analyticity of $u_\infty$ that $u_\infty$ is zero; therefore, $u$ vanishes outside $D$; in particular, $u \in \mathcal{W}$ is zero. □

**Remark 2.2.** *For the time-harmonic outgoing wave $u$, $(u,u)$ is a constant multiple of its energy flux over a period and through the $x$-axis. The naturally induced norm $\|u\| = (u,u)^{1/2}$ makes $\mathcal{W}$ a pre-Hilbert space.*

The next lemma is a direct consequence of the boundedness of the linear map $A$ and completeness of its domain $L^2(D)$.

**Lemma 2.3.** *The linear space $\mathcal{W}$ is complete, and therefore is a Hilbert space, with the inner product* (7).

**Remark 2.4.** *It follows from the boundedness of the kernel $H_0(k\rho)$ of the integral operator $A$ defined in* (5) *that the bounded linear map $A$ is compact, and has a singular value decomposition. It is not difficult to show that $A$ is compact when $D$ and the $x$-axis are not separated.*

**Remark 2.5.** *An orthogonal basis for $\mathcal{W}$ can be computed via the SVD of $A$. To construct an orthogonal basis in practice, the SVD will not be performed on $A$ for fear of inefficiency, but on a map related to standard layer-potentials, such as the combined-layer potential (see, for example,* [2]*, p. 47), whose domain is a set of functions defined on the boundary $\partial D$.*

## 3. The Inner Product for Two Point Sources

In this section, we calculate the inner product for wave functions each generated by a point source in $D$. This calculation on one hand will be useful for computing the SVD of $A$ or its equivalent layer potential representation (see Remark 2.5), on the other hand will demonstrate how an outgoing wave function from $D$ should be finitely sampled on $\mathbb{R}$.

### 3.1. **The inner product for two monopoles.**

We refer to the function $u(\mathbf{r}) = H_0(k|\mathbf{r} - \mathbf{r}'|)$ as the wave generated by a monopole at $\mathbf{r}' \in \mathbb{R}^2$.

**Theorem 3.1.** *Suppose that $u$, $v$ are generated by two monopoles at $\mathbf{b}$, $\mathbf{c} \in D$. Then the inner product $(u, v)$ depends only on the vector*

$$\mathbf{a} = \mathbf{b} - \mathbf{c} = (x_a, y_a). \tag{13}$$

*More precisely, let $a = |\mathbf{a}|$ and let $\phi = \arctan(y_a/x_a)$ be the angle formed by $x$-axis and $\mathbf{a}$. Then*

$$(u, v) = \frac{1}{\pi} \int_{-\pi/2}^{\pi/2} e^{-ika\,\sin(\theta-\phi)}\, d\theta. \tag{14}$$

*Thus $\mathrm{Re}(u, v) = J_0(k\,a)$ is independent of $\phi$. Furthermore, when $\mathbf{b} = \mathbf{c} \in D$,*

$$(u, u) = 1. \tag{15}$$

*Proof.* The proof follows that of Theorem 2.1 by replacing the integral along a segment of the $x$-axis with one along a semicircle in the lower half-plane,

$$\begin{aligned}(u, v) &= \lim_{r\to\infty} \frac{i}{4} \int_{-r}^{r} [u\bar{v}_n - \bar{v}u_n]\, dx \\ &= \lim_{r\to\infty} \frac{i}{4} \int_{\pi}^{2\pi} \left[ u(r,\theta) \frac{\partial \bar{v}(r,\theta)}{\partial r} - \bar{v}(r,\theta) \frac{\partial u(r,\theta)}{\partial r} \right] r\, d\theta,\end{aligned} \tag{16}$$

where the integrand of (16) is simplified by the far-field asymptotics of wave functions $u, v$ due to two monopoles.

1. **Geometry of the two sources.** We suppose that in cylindrical coordinates $\mathbf{r} = (r, \theta)$ with $\theta \in [\pi, 2\pi]$ and $\mathbf{b} = (b, \beta)$, $\mathbf{c} = (c, \gamma)$ with $\beta, \gamma \in (0, \pi)$; see Figure 3. The cosine law gives the distances $\rho = |\mathbf{r} - \mathbf{b}|$ and $\sigma = |\mathbf{r} - \mathbf{c}|$:

$$\rho^2 = b^2 + r^2 - 2br\cos(\theta - \beta) \tag{17}$$

$$\sigma^2 = c^2 + r^2 - 2cr\cos(\theta - \gamma). \tag{18}$$

From the pair of vertical sides and pair of horizontal sides of the dashed-line rectangle in Figure 3 we observe

$$\begin{aligned}-a\sin\phi &= c\sin\gamma - b\sin\beta \\ -a\cos\phi &= c\cos\gamma - b\cos\beta.\end{aligned}$$

We multiply the first equation by $-\cos\theta$, multiply the second by $\sin\theta$, and add to obtain

$$-a\sin(\theta - \phi) = c\sin(\theta - \gamma) - b\sin(\theta - \beta). \tag{19}$$

2. **Far-field asymptotics.** The monopoles are given by

$$u(\mathbf{r}) = H_0(k\rho), \qquad v(\mathbf{r}) = H_0(k\sigma) \tag{20}$$

with their normal derivatives given by

$$\frac{\partial u(\mathbf{r})}{\partial r} = -k\, H_1(k\rho)\, \frac{\partial \rho}{\partial r}, \qquad \frac{\partial v(\mathbf{r})}{\partial r} = -k\, H_1(k\sigma)\, \frac{\partial \sigma}{\partial r}. \tag{21}$$

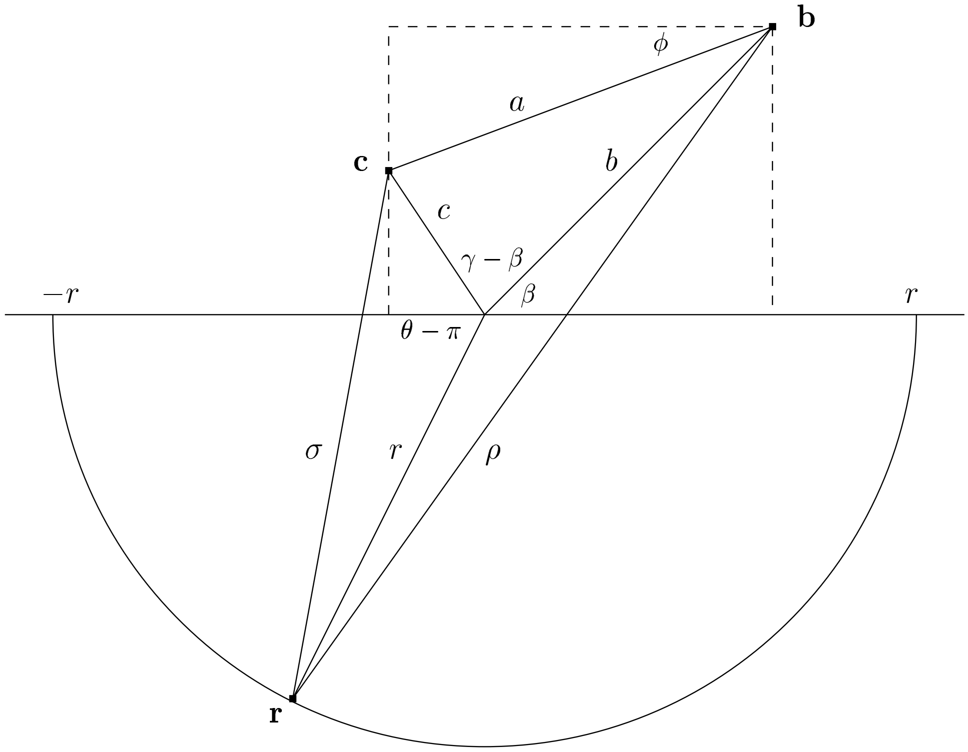


FIGURE 3. The source points $\mathbf{b}$ and $\mathbf{c}$ and field point $\mathbf{r}$, in cylindrical coordinates.

The derivatives $\partial\rho/\partial r$ and $\partial\sigma/\partial r$ both approach 1 as $r \to \infty$; since both terms of the integrand are bounded, these derivatives can be ignored. The large-argument asymptotic expansion for the Hankel functions (see, for example, [1], 9.2.3)

$$H_\nu(r) \sim \sqrt{2/(\pi r)}\, e^{i(r-\nu\pi/2-\pi/4)} + O(r^{-3/2}) \tag{22}$$

and the asymptotic expansion of $\rho$ and $\sigma$ from (17) and (18)

$$\rho \sim r - b\cos(\theta-\beta) + O(r^{-1}), \qquad \sigma \sim r - c\cos(\theta-\gamma) + O(r^{-1}) \tag{23}$$

as $r \to \infty$, combined with (16), (20), and (21) yield

$$(u, v) = \frac{1}{\pi}\int_{\pi}^{2\pi} e^{ik(c\cos(\theta-\gamma)-b\cos(\theta-\beta))}\, d\theta. \tag{24}$$

We shift the integration to $[-\pi/2, \pi/2]$ and employ (19) to obtain (14). $\square$

3.2. **The inner product for a monopole and a dipole.** Suppose that $u_{\mathbf{r}'}(\mathbf{r})$ is the wave function generated by a monopole at $\mathbf{r}' \in \mathbb{R}^2$, and $\mathbf{d} \in \mathbb{R}^2$ is a unit vector, with cylindrical coordinates $(1, \nu)$. Then the wave function generated by

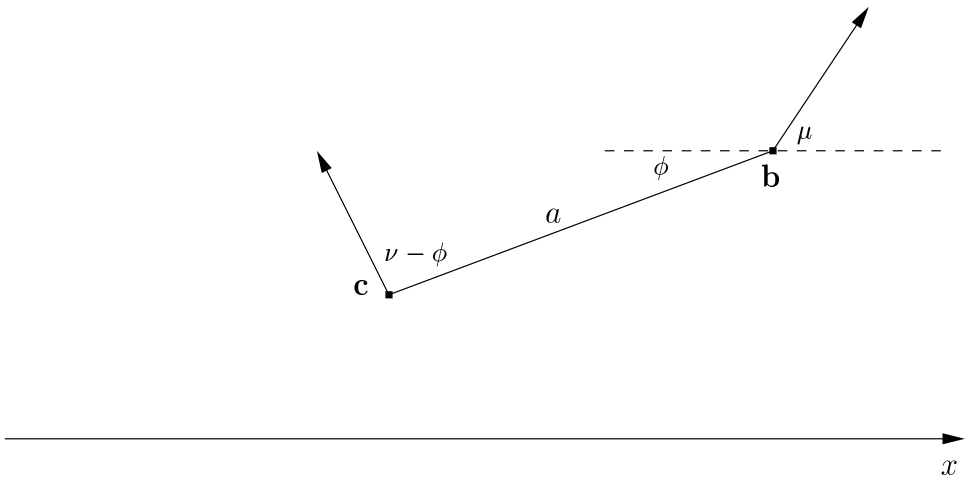


FIGURE 4. Two dipoles $\mathbf{b}$ and $\mathbf{c}$ with orientations $\mu$ and $\nu$.

a dipole at $\mathbf{r}'$ in orientation $\nu$ is defined as

$$\begin{aligned} v(\mathbf{r}) &= \lim_{t\to 0} \frac{u_{\mathbf{r}'}(\mathbf{r}+t\mathbf{d}) - u_{\mathbf{r}'}(\mathbf{r})}{t} \\ &= -\lim_{t\to 0} \frac{u_{\mathbf{r}'+t\mathbf{d}}(\mathbf{r}) - u_{\mathbf{r}'}(\mathbf{r})}{t}. \end{aligned} \tag{25}$$

**Theorem 3.2.** *Suppose that $u$, $v$ are generated by a monopole at $\mathbf{b} \in D$ and a dipole at $\mathbf{c} \in D$ with orientation $\nu$. Then the inner product $(u, v)$ depends on $\nu$ and the vector*

$$\mathbf{a} = \mathbf{b} - \mathbf{c} = (x_a, y_a). \tag{26}$$

*More precisely, let $a = |\mathbf{a}|$ and let $\phi = \arctan(y_a/x_a)$ be the angle formed by $x$-axis and $\mathbf{a}$. Then*

$$(u, v) = -\frac{ik}{\pi}\int_{-\pi/2}^{\pi/2} e^{-ika\,\sin(\theta-\phi)}\,\sin(\theta-\nu)\,d\theta. \tag{27}$$

*In particular, when $\mathbf{b} = \mathbf{c}$ and for arbitrary orientation $\nu$,*

$$(u, v) = -\frac{ik}{\pi}\int_{-\pi/2}^{\pi/2} \sin(\theta-\nu)\,d\theta = \frac{2ik}{\pi}\sin(\nu). \tag{28}$$

*Proof.* The proof exploits the definition of a dipole, the bilinearity of the inner product, and the inner product of two monopoles as derived above.

We define $\mathbf{c}_t = \mathbf{c} + t\mathbf{d}$, $\mathbf{a}_t = \mathbf{b} - \mathbf{c}_t$, $a_t = |\mathbf{a}_t|$, and $\phi_t$ to be the angle formed by the $x$-axis and $\mathbf{a}_t$. Referring to Figure 4, we observe

$$\begin{aligned} a_t &= a - t\cos(\nu - \phi) \\ \phi_t &= \phi - \arcsin\frac{t\sin(\nu-\phi)}{a_t}, \end{aligned}$$

from which

$$\lim_{t\to 0} \frac{a_t \sin(\theta-\phi_t) - a\sin(\theta-\phi)}{t} = \frac{d}{dt} a_t \sin(\theta-\phi_t)\Big|_{t=0} = -\sin(\theta-\nu). \tag{29}$$

Let $v_t$ denote a monopole located at $\mathbf{c}_t$. Then

$$(u,v) = -\lim_{t\to 0} \frac{(u,v_t)-(u,v_0)}{t}. \tag{30}$$

Combining (14) and (29) with (30) yields the desired result (27). □

3.3. **The inner product for two dipoles.** The computation of the inner product of two dipoles closely follows that of a monopole and dipole given above, yielding the following theorem.

**Theorem 3.3.** *Suppose that $u$, $v$ are generated by two dipoles at $\mathbf{b}$, $\mathbf{c} \in D$ with orientations $\mu$ and $\nu$. Then the inner product $(u,v)$ depends on the orientations and the vector*

$$\mathbf{a} = \mathbf{b} - \mathbf{c} = (x_a, y_a). \tag{31}$$

*More precisely, let $a = |\mathbf{a}|$ and let $\phi = \arctan(y_a/x_a)$ be the angle formed by $x$-axis and $\mathbf{a}$. Then*

$$(u,v) = \frac{k^2}{\pi}\int_{-\pi/2}^{\pi/2} e^{-ika\,\sin(\theta-\phi)} \sin(\theta-\mu)\,\sin(\theta-\nu)\,d\theta, \tag{32}$$

*where the unit vectors $\mu$ and $\nu$ are regarded as the angles they form with the $x$-axis; see Figure 4. In particular, when $\mathbf{b} = \mathbf{c} \in D$,*

$$(u,v) = \frac{k^2}{\pi}\int_{-\pi/2}^{\pi/2} \sin(\theta-\mu)\,\sin(\theta-\nu)\,d\theta = \frac{k^2}{2}\cos(\mu-\nu). \tag{33}$$

3.4. **The inner product for two multipoles.** We refer to the function $u(\mathbf{r}) = H_m(kr)\,e^{im\theta}$ as the wave generated by a multipole of order $m$ centered at $\mathbf{r}' \in \mathbb{R}^2$, where $\mathbf{r} - \mathbf{r}'$ has cylindrical coordinates $(r,\theta)$,

$$r = \left[(x-x')^2 + (y-y')^2\right]^{1/2}, \qquad \theta = \arctan\left[(y-y')/(x-x')\right]. \tag{34}$$

The inner product of two multipoles centered at $\mathbf{r}'$ has a very simple form.

**Theorem 3.4.** *Suppose that $u$, $v$ are generated by two multipoles of order $m$, $n$ centered at some point $\mathbf{r}'$ above the $x$-axis. Then*

$$(u,v) = \begin{cases} 1, & m = n, \\ 2(-1)^{(1+|m-n|)/2}/(|m-n|\pi), & m-n \text{ odd}, \\ 0, & \text{otherwise}. \end{cases} \tag{35}$$

*Proof.* The proof follows that of Theorem 3.1, except that the circular arc of radius $r$, below the $x$-axis, is centered at $\mathbf{r}' = (x', y')$. The multipoles are then given by

$$u(\mathbf{r}) = H_m(kr)\, e^{im\theta}, \qquad v(\mathbf{r}) = H_n(kr)\, e^{in\theta}, \tag{36}$$

their normal derivatives (see, for example, [1], 9.1.27) computed from

$$\frac{\partial H_m(kr)}{\partial r} = \frac{k}{2}\left(H_{m-1}(kr) - H_{m+1}(kr)\right), \tag{37}$$

and the asymptotic forms of the Hankel functions given by (22). Now we obtain

$$\begin{aligned}
(u, v) &= \lim_{r\to\infty} \frac{i}{4} \int_{\pi+\arcsin(y'/r)}^{2\pi-\arcsin(y'/r)} \left[ u(\mathbf{r}) \frac{\partial \bar{v}(\mathbf{r})}{\partial r} - \bar{v}(\mathbf{r}) \frac{\partial u(\mathbf{r})}{\partial r} \right] r\, d\theta \\
&= \lim_{r\to\infty} \frac{i}{4} \int_{\pi}^{2\pi} \left[ u(\mathbf{r}) \frac{\partial \bar{v}(\mathbf{r})}{\partial r} - \bar{v}(\mathbf{r}) \frac{\partial u(\mathbf{r})}{\partial r} \right] r\, d\theta \\
&= \frac{1}{\pi} \int_{\pi}^{2\pi} e^{i(m-n)(\theta-\pi/2)}\, d\theta,
\end{aligned}$$

from which the theorem is established. □

## 4. Other Unbounded Curves

The foregoing discussion has been limited to representation of the field of compact sources on a line. A review of the discussion reveals, however, that none of the argument is limited to a line: each fact applies equally to other curves that divide the plane into two unbounded regions, one of which contains the sources.

Let $C \subset \mathbb{R}^2$ be a curve with parametrization $\lambda : \mathbb{R} \to \mathbb{R}^2$, so that $\lambda(t) \in C$ for $t \in \mathbb{R}$. We suppose that $C$ is simple ($\lambda$ is a one-to-one map), that $C$ is unbounded ($|\lambda(t)| \to \infty$ as $t \to \pm\infty$), and $C$ carves out a sector of the plane,

$$\lim_{t\to-\infty} \frac{\lambda(t)}{|\lambda(t)|} = \mathbf{d}_-, \qquad \lim_{t\to\infty} \frac{\lambda(t)}{|\lambda(t)|} = \mathbf{d}_+, \tag{38}$$

for some $\mathbf{d}_-, \mathbf{d}_+$. Under these assumptions, $C$ divides the plane into two regions. If $u, v$ are waves whose sources lie entirely in the same region, the bilinear form

$$(u, v) = \frac{i}{4} \int_C [u\, \bar{v}_n - \bar{v}\, u_n]\, d|C| \tag{39}$$

is independent of $C$ other than the unit vectors $\mathbf{b}$ and $\mathbf{c}$. Furthermore $(u, u)$ is positive for $u \neq 0$, provided that the direction of the normal to $C$ is chosen to point away from the source region, the integration is taken in the counterclockwise direction relative to the sources, and $\mathbf{b} \neq \mathbf{c}$. Hence, under these conditions, the bilinear form is an inner product. We remark that the plane could alternatively be divided into regions by a curve $C$ satisfying (38) with $\mathbf{b} = \mathbf{c}$, giving an infinite enclosed strip. In this case, if the sources are in the strip, then the bilinear form is an inner product, whereas if the sources are outside, then $(u, u) = 0$ for all waves $u$.

The follow theorem restates the results of the previous section for the inner products of point sources, for a simple, unbounded curve of the type just presented. Its proof exactly follows those for the line and is omitted.

**Theorem 4.1.** *Suppose that $C$ is an unbounded curve dividing the plane into two regions and $(u, v)$ is the inner product defined by (39), where $u, v$ are point sources located at $\mathbf{b}, \mathbf{c}$ lying in one of the regions. Suppose $\beta$ and $\gamma$ are the orientations of the unit vectors $\mathbf{d}_-, \mathbf{d}_+$ given in (38), where $\lambda(t)$ traverses $C$ counterclockwise, for increasing $t$, relative to $\mathbf{b}$ and $\mathbf{c}$. Finally, suppose $\mathbf{a} = \mathbf{b} - \mathbf{c} = (x_a, y_a)$, $a = |\mathbf{a}|$, and $\phi = \arctan(y_a/x_a)$.*

*1.* **Inner product of two monopoles.** *If $u, v$ are monopoles, then*

$$(u, v) = \frac{1}{\pi} \int_\beta^\gamma e^{-ika\cos(\theta-\phi)}\, d\theta. \tag{40}$$

*2.* **Inner product of a monopole and a dipole.** *If $u$ is a monopole and $v$ is a dipole with orientation $\nu$, then*

$$(u, v) = \frac{k}{\pi} \int_\beta^\gamma e^{-ika\cos(\theta-\phi)} \cos(\theta - \nu)\, d\theta. \tag{41}$$

*3.* **Inner product of two dipoles.** *If $u, v$ are dipoles with orientations $\mu, \nu$, then*

$$(u, v) = \frac{k^2}{\pi} \int_\beta^\gamma e^{-ika\cos(\theta-\phi)} \cos(\theta - \nu) \cos(\theta - \mu)\, d\theta. \tag{42}$$

*4.* **Inner product of two multipoles.** *If $\mathbf{b} = \mathbf{c}$ and $u, v$ are multipoles of order $m, n$, then*

$$(u, v) = \frac{1}{\pi} \int_\beta^\gamma e^{i(m-n)(\theta-\pi/2)}\, d\theta. \tag{43}$$

## 5. Analytical and Numerical Examples

While we defer actual applications to subsequent work, here we present examples illustrating how the inner product can be used to construct a basis.

We can obtain the singular value decomposition of the operator $A : L^2(D) \to C^\infty(\mathbb{R})$ of Section 2 from the eigendecomposition of a truncated $N \times N$ *Gram matrix* of inner products $B = \{(u_m, u_n)\}$, where $u_n = Ae_n$ and $\{e_n,\ n \in \mathbb{Z}\}$ is an orthonormal basis for $L^2(D)$. (This procedure "squares the system," so is not advisable in some applications.) In particular, suppose $B = WDW^h$, where $W$ is unitary and $D$ is diagonal. If $w_i$ and $w_j$ are two columns of $W$, with $w_i = \langle w_{1i}, \ldots, w_{Ni}\rangle^t$ and $w_j = \langle w_{1j}, \ldots, w_{Nj}\rangle^t$, then we define image-space functions $s_i = \sum_k w_{ki}\, u_k$ for $i = 1, \ldots, n$, and obtain

$$(s_i, s_j) = \sum_{k=1}^{n} \sum_{l=1}^{n} w_{ki}\, \bar{w}_{lj}\, (u_k, u_l) = {w_j}^h\, B\, w_i = \delta_{ij}\, d_i, \tag{44}$$

where $d_i$ is the $i$th element on the diagonal of $D$. Thus $\{s_1, \ldots, s_N\}$ is an orthogonal set in the image space with $(s_i, s_i) = d_i$.

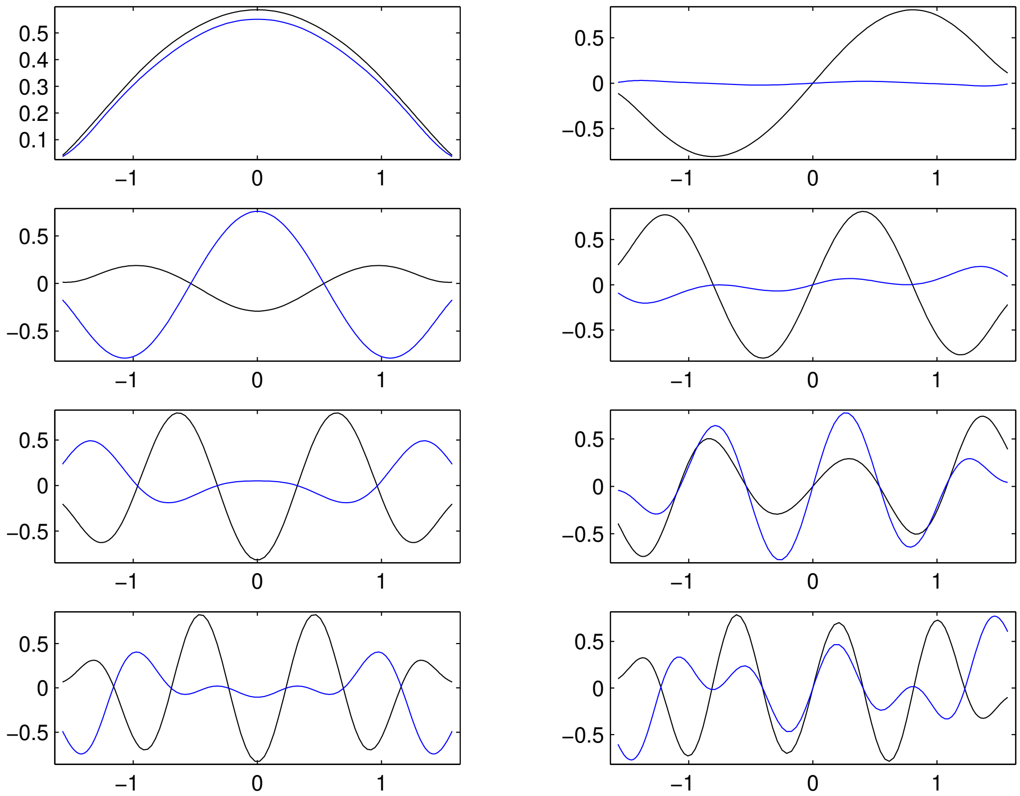


FIGURE 5. Singular functions $v_1, \ldots, v_8$ from Example 1 for $k = 10$ are shown, each divided by monopole $u_0$ to normalize scale and oscillations. They are plotted along the entire $x$-axis as a function of $\theta \in [-\pi/2, \pi/2]$ with $x = y_0 \tan\theta$. Real, imaginary parts shown.

In the examples, we replace the map $A$ from the source region (to the field region) by a map $\tilde{A}$ from the boundary of the source region, which is sufficient and simplifies the analysis. In the domain we will have Dirichlet data (Examples 1 and 2) or a single-layer density (Examples 3 and 4), and, in a slight abuse of notation, we use $\tilde{A}$ to denote the operator in each case.

**Example 1.** Suppose all sources are contained within a disk $D$ of radius $r_0$ centered at $\mathbf{r}' = (0, y_0)$ with $y_0 > r_0$. Complex exponentials $\{e_n(\theta) = e^{in\theta},\ n \in \mathbb{Z}\}$

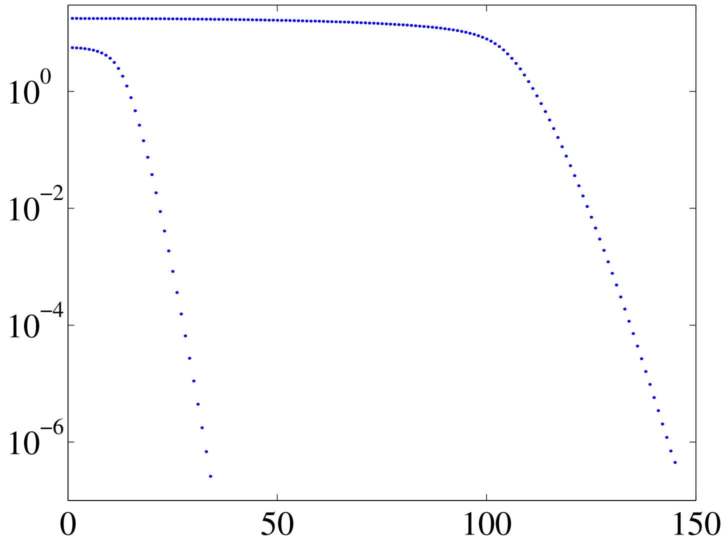


FIGURE 6. The singular values of the operator $A$ in Example 1 are shown on a log scale, in decreasing order, for $k = 10$ (shorter sequence) and $k = 100$.

form an orthonormal basis for $L^2(\partial D)$ under the usual inner product. The map $\tilde{A}:\ L^2(\partial D) \to C^\infty(\mathbb{R})$ is given by

$$u_n(x) = (\tilde{A}e_n)(x) = \frac{H_n(kr)}{H_n(kr_0)}\, e^{in\theta}, \qquad n \in \mathbb{Z}, \tag{45}$$

where $r = \sqrt{x^2 + {y_0}^2}$ and $\theta = \arctan(-y_0/x)$. From Theorem 3.4,

$$(u_m, u_n) = \frac{1}{H_m(kr_0)\bar{H}_n(kr_0)} \begin{cases} 1, & m = n, \\ 2(-1)^{(1+|m-n|)/2}/(|m-n|\pi), & m-n \text{ odd}, \\ 0, & \text{otherwise}. \end{cases}$$

For $r_0 = 1$, $y = 3/2$, and $k = 10$, we truncate the matrix $B = \{(u_m, u_n)\}$ at $|n| \le n_{\max} = 25$ ($N = 51$), for which all eigenvalues $d_1 > \cdots > d_N$ agree with other truncations with $n_{\max} > 25$ to within $5 \cdot 10^{-15}$. Here $d_1 = 31.3$ and $d_{35} = 9.97 \cdot 10^{-15}$; the singular values $\sqrt{d_1}, \ldots, \sqrt{d_{35}}$ are shown in Figure 6. Image-space singular functions $v_i = s_i/\sqrt{d_i}$ for $1, \ldots, 8$ are plotted in Figure 5.

The analogous computation was done for $k = 100$, for which $n_{\max} = 135$ suffices. Singular values $\sqrt{d_1}, \ldots, \sqrt{d_{145}}$ are shown with those for $k = 10$ in Figure 6 and the singular functions $v_1, \ldots, v_8$ are plotted in Figure 7.

**Example 2.** We suppose again that all sources are contained within a disk $D$ of radius $r_0$ and ask about the singular functions on two horizontal lines, one above and one below $D$. This is the limiting case of an enclosing rectangle of fixed height and increasing width. Reasoning from Green's second theorem (as in Theorem 2.1) we observe that two wave functions $u, v$ from sources inside $D$ have inner product $(u, v)$ that is invariant through the limiting process; in fact

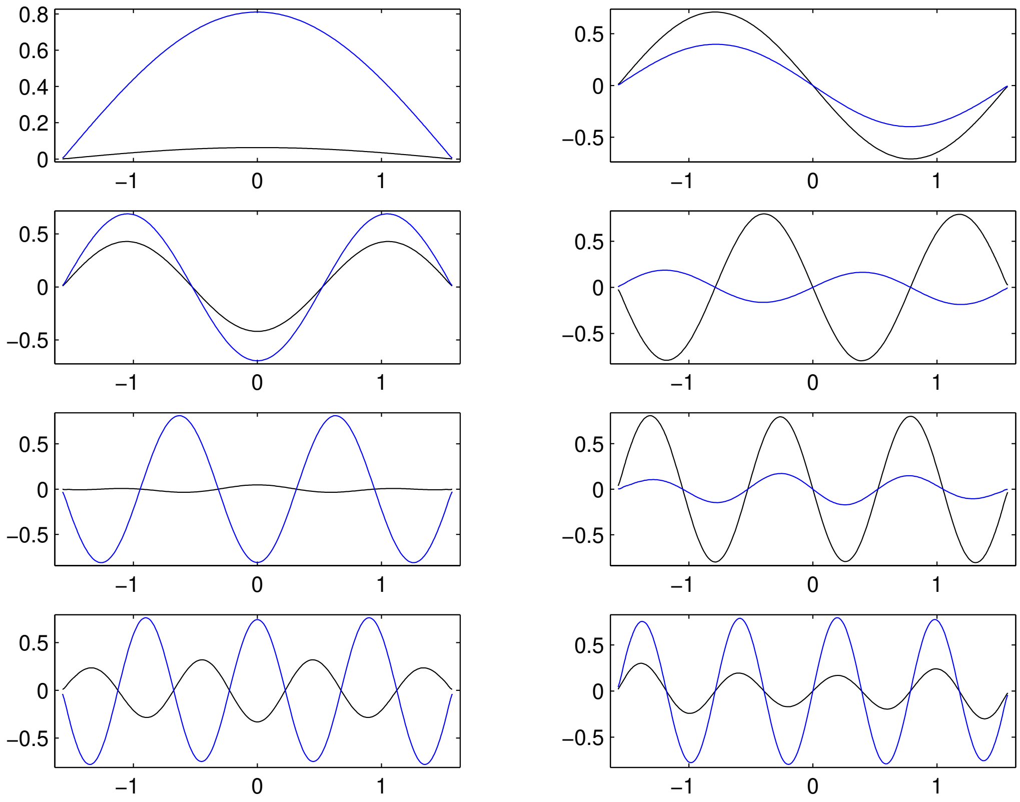

FIGURE 7. Singular functions as in Figure 5, but for $k = 100$.

it can be computed most simply on the boundary $\partial D$. For multipole sources

$$u_n(\mathbf{r}) = H_n(k|\mathbf{r} - \mathbf{r}'|)\, e^{in\theta}, \qquad n \in \mathbb{Z}, \tag{46}$$

at the center $\mathbf{r}'$ of $D$, we obtain

$$(u_m, u_n) = 2\,\delta_{mn}. \tag{47}$$

(On $\partial D$ the integrand of the inner product is a constant times $e^{i(m-n)\theta}$, so $(u_m, u_n) = c_n\,\delta_{mn}$. Now employ Theorem 3.4 or, more directly, the Wronskian for $H_n$.) Thus the multipoles, scaled by $1/\sqrt{2}$, form an orthonormal basis on the two parallel lines.

Although the multipole $u_n$ "radiates energy" that is invariant with $n$, its field values grow exponentially in $n$ on $\partial D$ for $|n| > kr_0$. The exponential growth typically makes multipoles an unsuitable basis for a source region very different from a disk.

**Example 3.** Next we consider sources inside a rectangular region

$$R = \{(x, y) : \; |x| \le a, \; |y - y_0| \le b\}, \qquad y_0 > b. \tag{48}$$

Outside $R$ we represent the waves with a single-layer potential, arising from a density $\eta$ on the boundary $\partial R$. The density is discretized on each edge of

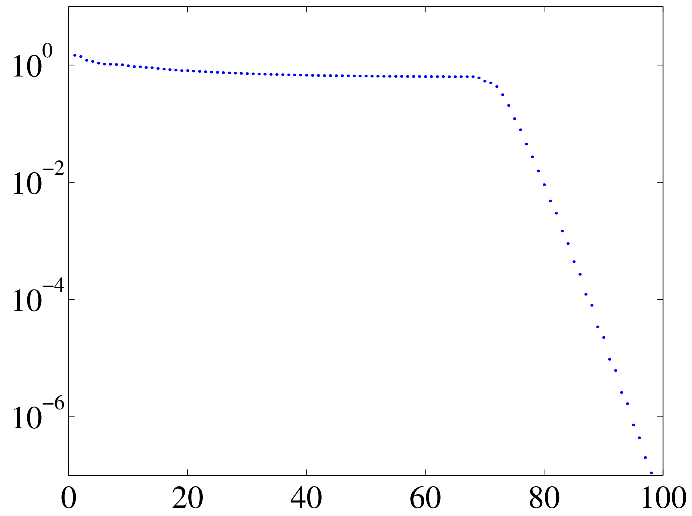


FIGURE 8. The singular values of the operator $A$ in Example 3.

the rectangle with Gauss-Legendre quadrature, yielding a set of monopoles as sources. This choice of discretization of the source region is not optimal, but the size of the basis is within about a factor of three of optimal. (In an optimal discretization the nodes would be spaced nearly uniformly on the edges similar to nodes for bandlimited functions; see [3]). Furthermore, the eigendecomposition of the Gram matrix yields an optimal basis in the image space.

For $a = 10$, $b = 1$, $y_0 = 3/2$, and $k = 10$, we choose 150 nodes on the horizontal edges and 20 nodes on the vertical edges, so $N = 340$. The integral (14) for the inner product of monopoles is discretized here with Gauss-Legendre quadrature containing 250 nodes. The singular values $\sqrt{d_1}, \ldots, \sqrt{d_{98}}$ of the operator $\tilde{A} : L^2(\partial R) \to C^\infty(\mathbb{R})$ are plotted in Figure 8. Figure 9 shows the first two image-space singular functions $v_1, v_2$ and the integrands on the $x$-axis of the corresponding inner products $(v_1, v_1)$ and $(v_2, v_2)$. Due to the elongated source region, division by a monopole centered at the source center $(0, y_0)$ does not eliminate oscillations in the singular functions.

**Example 4.** In our final example we examine the possibility of a source being focused to maximize or minimize the radiated energy that passes through a particular segment in the finite plane. We again let the source be the rectangular region $R$ of Example 3, and the target be the segment

$$T = \{(x, y) : |x| \leq c, \ y = y_0 - r\}, \tag{49}$$

where we let $c = 1$ and $r$ be a variable parameter.

The inner product presented above lacks positivity on finite curves and in this setting is merely a bilinear form. No analytical formula for its value is available in this case; both the source region and the target region must be discretized. Again we choose $k = 10$, discretize the source region as for Example 3, and apply Gauss-Legendre quadrature (with 20 nodes) on the target segment. As in previous examples we obtain the eigendecomposition of the matrix $\{(u_m, u_n)\}$, where $u_m$ is the wave due to a monopole on $\partial R$.

In Figure 10 the maximum and minimum values of the bilinear form $(u, u)$, for unit preimage are shown, as a function of $r$. Note that the minimum value is negative throughout the range of $r$. Figure 11 shows for $r = 2$ the waveform and the integrand of the bilinear form for the source with the maximum radiation through the target segment.

## 6. Generalizations and Conclusions

The inner product generalizes immediately to three dimensions; a paper describing corresponding analytical and computational tools is in preparation.

Exploitation of the inner product in applications remains to be described, but initial explorations provide encouragement that it will prove to be of fundamental value for problems in both acoustics and electromagnetics, scattering and inverse scattering.

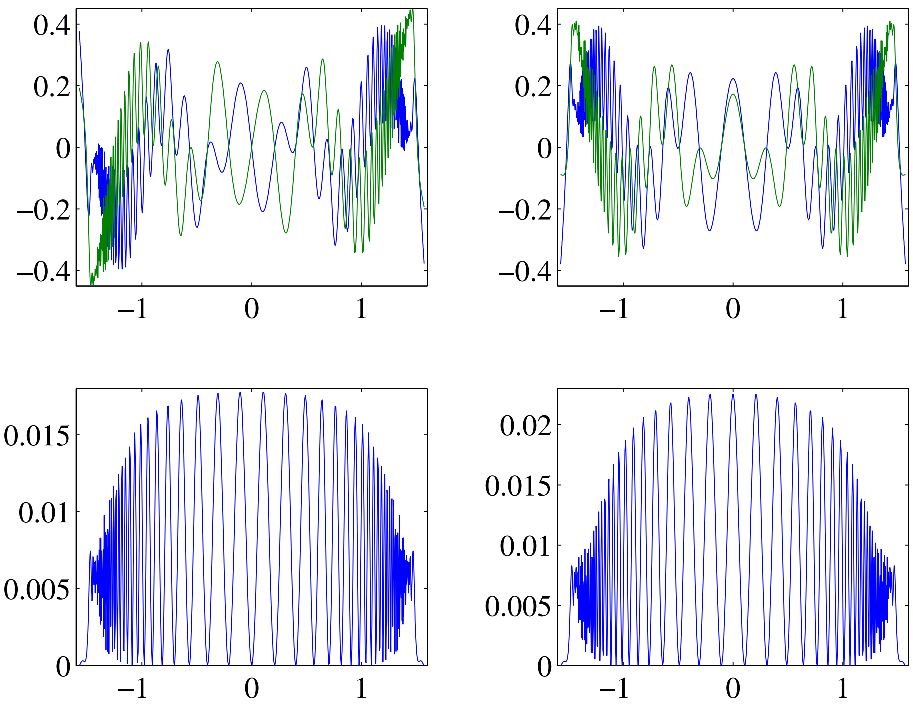


Figure 9. Singular functions $v_1, v_2$, divided by the monopole centered at $(0, y_0)$ (top), and integrands of the corresponding inner products $(v_i, v_i)$ for $i = 1, 2$ (bottom) from Example 3 are shown. As for Figure 5, they are plotted as a function of $\theta \in [-\pi/2, \pi/2]$ with $x = y_0 \tan\theta$.

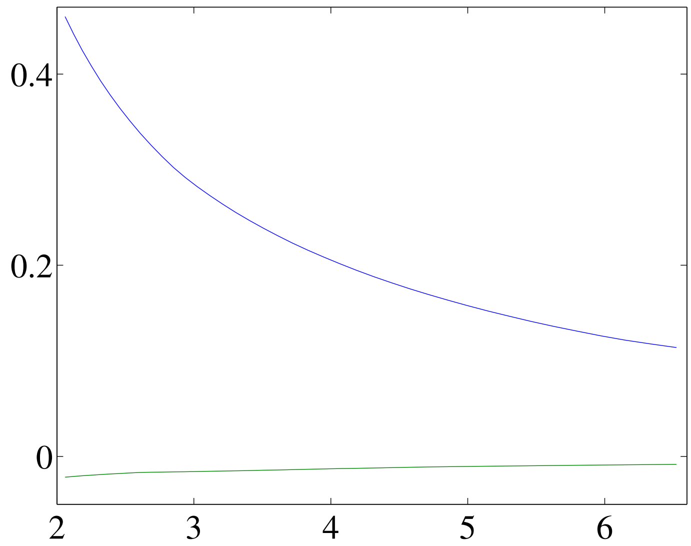


FIGURE 10. The maximum and minimum radiated energy through a segment as a function of distance $r$ to the source (Example 4).

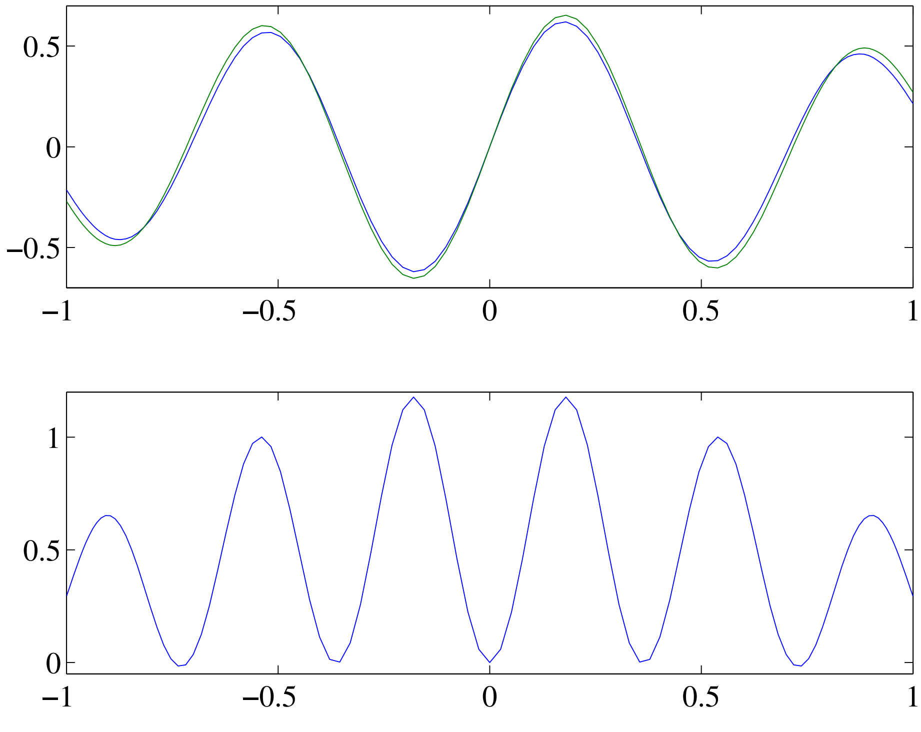


FIGURE 11. Waveform having maximum radiated energy (above) and the corresponding integrand of the bilinear form (below) for $r = 2$ in Example 4.

## REFERENCES

[1] Abramowitz, M. and Stegun, I., *Handbook of Mathematical Functions* (10th printing), National Bureau of Standards (U.S.), Applied Mathematics Series 55 (1972).

[2] Colton, D. and Kress, R., *Inverse Acoustic and Electromagnetic Scattering Theory,* Applied Mathematical Sciences **93**, Springer, Berlin (1992).
[3] Xiao, H., Rokhlin, V., and Yarvin, N., "Prolate spheroidal wavefunctions, quadrature and interpolation," *Inverse Problems* **17** (4), 805-838 (2001).

National Institute of Standards and Technology, 325 Broadway, Boulder, CO 80305-3328
*E-mail address*: `alpert@boulder.nist.gov`

Courant Institute of Mathematical Sciences, New York University, 251 Mercer Street, New York, NY 10012-1110
*E-mail address*: `yuchen@cims.nyu.edu`